



Published in final edited form as:

J Neurosci. 2012 October 17; 32(42): 14557–14562. doi:10.1523/JNEUROSCI.0559-12.2012.

Phosphorylation of adenylyl cyclase III at serine¹⁰⁷⁶ does not attenuate olfactory response in mice

Katherine D Cygnar, Sarah Ellen Collins, Christopher H Ferguson, Chantal Bodkin-Clarke, and Haiqing Zhao

Biology Department, Johns Hopkins University 3400 N. Charles Street, Baltimore, MD 21218

Abstract

Feedback inhibition of adenylyl cyclase III (ACIII) via Ca²⁺-induced phosphorylation has long been hypothesized to contribute to response termination and adaptation of olfactory sensory neurons (OSNs). To directly determine the functional significance of this feedback mechanism for olfaction *in vivo*, we genetically mutated serine¹⁰⁷⁶ of ACIII, the only residue responsible for Ca²⁺-induced phosphorylation and inhibition of ACIII (Wei et al., 1996; Wei et al., 1998), to alanine in mice. Immunohistochemistry and Western blot analysis showed that the mutation affects neither the ciliary localization nor the expression level of ACIII in OSNs.

Electroolfactogram analysis showed no differences in the responses between wildtype and mutant mice to single-pulse odorant stimulations or in several stimulation paradigms for adaptation. These results suggest that phosphorylation of ACIII on serine¹⁰⁷⁶ plays a far less important role in olfactory response attenuation than previously thought.

Introduction

In vertebrates, olfactory sensory neurons (OSNs) in the nose use a cyclic AMP (cAMP)-mediated signaling pathway to transform odor stimulation into electrical neural signals. Odor exposure leads to activation of adenylyl cyclase III (ACIII) on OSN cilia (Bakalyar and Reed, 1990; Wong et al., 2000) and elevation of ciliary cAMP levels. cAMP in turn binds and opens the olfactory cyclic nucleotide-gated (CNG) cation channel, resulting in influx of Ca²⁺ and Na⁺ and subsequent membrane depolarization. Ca²⁺ then contributes to further membrane depolarization by triggering efflux of Cl⁻ through opening the olfactory Ca²⁺-activated Cl⁻ channel ANO2 (Stephan et al., 2009; Billig et al., 2011) (for review see Firestein (2001) (Firestein, 2001) and Kleene (2008) (Kleene, 2008)).

OSNs, like other sensory receptor cells, exhibit reduced sensitivity upon sustained or repeated stimulation—a phenomenon known as adaptation. Ca²⁺, in addition to mediating membrane depolarization, has been demonstrated to be the key mediator for OSN adaptation (Kurahashi and Shibuya, 1990; Leinders-Zufall et al., 1998; Stephan et al., 2012), presumably through negative regulation of activities of several components in the olfactory signal transduction pathway (Zufall and Leinders-Zufall, 2000).

One prominent target of the negative feedback by Ca²⁺ is ACIII. Firstly, when heterologously expressed in HEK293 cells, ACIII is inhibited by elevated intracellular Ca²⁺ levels. This Ca²⁺-induced ACIII inhibition results from phosphorylation by Ca²⁺/calmodulin-dependent protein kinases II (CaMKII) (Wayman et al., 1995; Wei et al., 1996).

Corresponding Author: Haiqing Zhao hzhao@jhu.edu Biology Department, Johns Hopkins University 3400 N. Charles Street, Baltimore, MD 21218.

Conflict of Interest Statement: The authors declare they have no competing interests

A single amino acid, serine¹⁰⁷⁶, of ACIII is identified to be the only phosphorylation site responsible for Ca²⁺-induced inhibition. Mutating serine¹⁰⁷⁶ to alanine abolishes Ca²⁺-induced phosphorylation of ACIII as well as the activity inhibition (Wei et al., 1996). Secondly, in preparations of olfactory cilia, elevated Ca²⁺ levels reduce odorant- or forskolin-induced cAMP production (Boekhoff et al., 1996), and CaMKII inhibitors prolong odorant-induced cAMP transients (Wei et al., 1998). Consistently, odorants induce phosphorylation of ACIII at serine¹⁰⁷⁶, and this phosphorylation is blocked by CaMKII inhibitors (Wei et al., 1998). Finally, in isolated OSNs, electrophysiological recordings show that CaMKII inhibitors impair adaptation during or following sustained odorant stimulation, but has little effect on adaptation induced by brief odorant stimulation (Leinders-Zufall et al., 1999). Combined, these observations have led to a hypothesis that feedback inhibition of ACIII via Ca²⁺-induced phosphorylation by CaMKII serves as a mechanism to attenuate OSN responses, particularly for adaptation induced by sustained odor stimulations (Wei et al., 1998; Leinders-Zufall et al., 1999; Zufall and Leinders-Zufall, 2000). This hypothesis, however, has not been directly tested *in vivo*. Whether and to what extent Ca²⁺-induced ACIII phosphorylation may contribute to olfactory response attenuation remains unknown.

To directly assess the contributions of Ca²⁺-induced phosphorylation of ACIII to olfactory response, we generated a mouse strain carrying a modified version of ACIII, in which the key serine¹⁰⁷⁶ phosphorylation site is mutated to alanine. Electrophysiological analysis revealed no differences in the response properties between wildtype and mutant mice to single-pulse stimulations and in several adaptation paradigms. These results suggest that phosphorylation of ACIII at serine¹⁰⁷⁶ is not necessary for olfactory adaptation to occur.

Materials and Methods

For all experiments, mice were handled and euthanized with methods approved by the Animal Care and Use Committees of Johns Hopkins University (JHU).

Gene targeting

In the mouse, *Adcy3* gene is located on chromosome 12 and encodes ACIII protein of 1145 amino acids. *Adcy3* consists of 22 exons, and the coding sequence for the CaMKII phosphorylation site, serine¹⁰⁷⁶, is in exon 21. Homologous recombination with the targeting vector introduced a T->G point mutation in *Adcy3* exon 21 and inserted a self-excising neomycin (neo) selection cassette (Bunting et al., 1999) 81 base pairs downstream of exon 21 splice donor in intron 21-22. The T->G mutation changes codon 1076 from TCC, encoding serine, to GCC, encoding alanine. The targeting vector was constructed from DNA fragments amplified by high fidelity PCR from 129/Sv mouse genomic DNA followed by PCR-based site directed mutagenesis, and was then linearized and electroporated into mouse ES cells (MC1 clone, JHU transgenic facility). Homologous recombination events were screened by PCR of genomic DNA with primer pairs that span the homologous arms. Injection of modified ES cells into C57BL/6 blastocysts to generate chimeric offspring was performed at JHU Transgenic Facility. Chimeric males were mated to C57BL/6 females to obtain germline transmission. The neo cassette was removed via cre-mediated excision in the male germline of chimeric mice to leave a single LoxP site in intron 21-22.

Immunohistochemistry

Anesthetized mice were perfused transcardially with 1X PBS followed by 4% (wt/vol) paraformaldehyde. Olfactory tissues were dissected and postfixed for 2 hrs at 4°C followed by cryoprotection in 30% (wt/vol) sucrose overnight at 4°C. Cryosections were cut 14 μm thick and stored at -80°C. Tissue sections were incubated overnight at 4°C with primary antibodies in 1x PBS containing 0.1% (vol/vol) Triton X-100 and 1% (vol/vol) normal

donkey serum. After washing, the sections were incubated with secondary antibodies conjugated to Alexa-488, or -546, or -647 (Molecular Probes) and imaged by confocal microscopy (LSM 510 Meta, Zeiss). Primary antibodies were used at the following dilutions: anti-PDE1C2 (provided by Dr. J. Beavo), 1:500; anti-PDE4A (provided by Dr. J. Cherry), 1:200; anti-CNGB1 (Song et al., 2008), 1:200; anti-ACIII (Santa Cruz SC-588), 1:200; anti-OMP (provided by Dr. F. Margolis), 1:1000; anti-Gap43 (Chemicon MAB347), 1:500; anti-acetylated tubulin (Sigma T7451), 1:500.

Western blotting

Olfactory epithelium (OE) was dissected and homogenized in 2x Laemmli buffer and stored at -80°C . Tissue homogenates were subjected to SDS-PAGE followed by transferring onto PVDF membrane. Membranes were incubated with blocking buffer (5% (wt/vol) non-fat dry milk in TBST (20 mM Tris, 150 mM NaCl, and 0.1% (vol/vol) Tween-20)) for 1 hr at room temperature and then incubated overnight at 4°C with primary antibodies at respective dilutions in blocking buffer. Membranes were then washed with TBST followed by incubation with secondary antibodies conjugated to HRP in blocking buffer for 1 hr at room temperature. The blot was visualized with ECL Plus reagent (GE Life Sciences) with detection on a Typhoon 9410 Variable Mode Imager. Band density was quantified using ImageJ. Primary antibodies were used at the following dilutions: anti-PDE1C, 1:5000; anti-PDE4A, 1:5000; anti-CNGB1, 1:2000; anti-ACIII, 1:1000; anti-alpha tubulin (Sigma T8203), 1:10,000.

Electroolfactogram (EOG)

EOG recording was performed as previously described (Cygnar et al., 2010). The mouse was sacrificed by CO_2 asphyxiation and decapitated. The head was cut sagittally to expose the medial surface of the olfactory turbinates. The recording electrode, a Ag-AgCl wire in a capillary glass pipette filled with Ringer solution (in mM: 135 NaCl, 5 KCl, 1 CaCl_2 , 1.5 MgCl_2 , 10 HEPES, pH 7.4) containing 0.5% agarose, was placed on the surface of the OE and connected to a differential amplifier (DP-301, Warner Instruments). EOG signals were recorded from the surface of turbinate IIB and acquired and analyzed with AxoGraph software (Axon Instruments) on a Macintosh computer. The signals were filtered DC - 1 kHz and recorded at a sampling rate of 2 kHz. The recorded signals were low-pass filtered at 25 Hz during analysis. Odorant solutions were prepared as 0.5 M stocks in dimethyl sulfoxide and were then diluted with water to the concentration for EOG recording. Vapor-phase odorant stimuli were generated by placing 5 ml of odorant solution in a sealed 60 ml glass bottle. This vapor is delivered by a Picospritzer (Parker Hannifin) as a pulse injected into a continuous stream of humidified air flowing over the tissue sample. All EOG recordings were conducted at room temperature and in mice older than 6 weeks.

Statistical analysis

All statistical significance was determined by unpaired t-test.

Results

Generation of ACIII^{S1076A} mice

To eliminate Ca^{2+} -induced phosphorylation of ACIII in OSNs, we generated a mouse strain, ACIII^{S1076A}, in which the codon for serine¹⁰⁷⁶ (TCC) of the *Adcy3* gene was mutated to a codon for alanine (GCC) via homologous recombination (Fig. 1A). A self-excising neomycin selection cassette (Bunting et al., 1999) is inserted downstream of exon 21 to allow for selection of homologous recombination events in the embryonic stem cells. The neomycin cassette is removed via cre-mediated recombination in the male germline, leaving

a single loxP site in intron 21-22 and allowing minimal disruption of the *adcy3* gene. The T->G mutation in the genomic DNA was confirmed in mice homozygous for the targeted allele by sequencing of a PCR product spanning the mutated exon and the remaining loxP site (Fig. 1B).

The ACIII^{S1076A} mice are viable and have no overt developmental and behavioral abnormalities. Cryosectioning and immunostaining analysis showed that the olfactory epithelium (OE) of ACIII^{S1076A} mice has no differences from that of wildtype mice in gross morphology, and that ACIII and other olfactory signal transduction components including the CNG channel subunit CNGB1b and phosphodiesterase 1C (PDE1C) are all located at the ciliary layer of the OE in ACIII^{S1076A} mice, similar to wildtype mice (Fig. 1C). Western blotting against ACIII on OE extracts showed that the amount of ACIII protein in the ACIII^{S1076A} OE is comparable to that in the wildtype mice (Fig. 1D). We conclude that the mutation introduced into *Adcy3* does not affect the expression and localization of the mutant protein.

Responses to single odorant pulses are comparable in wildtype and ACIII^{S1076A} mice

To assess the responses to odor in ACIII^{S1076A} mice, we performed electroolfactogram (EOG) analysis (Scott and Scott-Johnson, 2002; Cygnar et al., 2010). All EOG recordings were carried out using both amyl acetate and heptaldehyde as stimulating odorants, and the results were similar for both odorants. For simplicity, we present only the recordings using amyl acetate.

We first recorded the OSN response to brief (100 msec) odorant pulses. ACIII^{S1076A} OSNs showed similar response amplitude to wildtype OSNs across a range of odorant concentrations (Fig. 2A). The response of ACIII^{S1076A} OSNs to amyl acetate at 10⁻² M, a near saturating concentration for EOG, was 19.9 ± 1.9 mV (n = 5 mice, range is 95% CI), which is comparable to the wildtype response of 18.9 ± 2.8 mV (n = 4 mice, 95% CI). ACIII^{S1076A} OSNs also showed no differences compared to wildtype in response kinetics to single 100-msec pulses of odorants (Fig. 2B-D). The time-to-peak of the EOG signal for amyl acetate at 10⁻⁴ M, a near EC₅₀ concentration of the dose-response relation, was 366 ± 18 msec (n = 8 mice, 95% CI) for ACIII^{S1076A} mice as compared to 364 ± 21 msec (n = 8 mice, 95% CI) for wildtype mice. Thus, phosphorylation of ACIII on serine¹⁰⁷⁶ is not a determinant for the sensitivity and kinetics of OSN responses to short odorant pulses.

We then examined the response to a sustained (10 sec) pulse of odorant. CaMKII inhibitors attenuate desensitization during sustained (8 sec) odorant stimulation in newt OSNs (Leinders-Zufall et al., 1999); however, ACIII^{S1076A} OSNs showed similar desensitization to wildtype OSNs as measured by the percent reduction in response over the duration of the stimulation (Fig. 2E,F). For amyl acetate at 10⁻⁴ M, the amplitude of EOG signal at the end of the stimulation reduced to 55% of the peak value in ACIII^{S1076A} mice as compared to 53% in wildtype mice. We conclude that phosphorylation of ACIII on serine¹⁰⁷⁶ is not required for desensitization during sustained odorant stimulation.

ACIII^{S1076A} mice show no adaptation defects in brief or sustained paired-pulse stimulation paradigms

To assess the ability of ACIII^{S1076A} OSNs to adapt to odorant stimulation, we recorded EOG using several adaptation stimulation paradigms. Because CaMKII inhibitors impair adaptation following sustained (8 sec) but not brief odorant pulses (Leinders-Zufall et al., 1999), we first examined responses to paired sustained odorant pulses (Fig. 3A). In such paired-pulse paradigm, the OE was subject to a 10-sec odorant pulse followed by a 5-sec pulse of the same concentration after a 2-sec interpulse interval. Adaptation induced by the

1st sustained odorant pulse manifests in the response to the 2nd pulse as both amplitude reduction and activation kinetics slowing down. In ACIII^{S1076A} mice, the EOG signal of the 2nd pulse displayed an amplitude reduction comparable to that of wildtype mice (Fig. 3A,B) in all odorant concentrations tested. Similarly, slowed activation kinetics, quantified as the lengthening of the time-to-peak, in ACIII^{S1076A} mice is comparable to that of wildtype mice (Fig. 3C,D). We further examined adaptation during a train of brief odorant pulses, a stimulation paradigm resembling the pattern of breathing. The OE was subject to a train of 100-msec pulses (30 total) with a 0.5-sec interpulse interval between each pulse (Fig. 3E). ACIII^{S1076A} OSNs showed a response pattern indistinguishable to that of wildtype OSNs in all odorant concentrations tested (Fig. 3E,F). Together, these data suggest that phosphorylation of ACIII on serine¹⁰⁷⁶ is not required for proper adaptation induced by either brief or sustained odorant stimulations.

Discussion

Adaptation is a common feature of sensory transduction, and allows sensory receptor cells to code a wide dynamic range of sensory stimuli by resetting the stimulation–response relationship. Understanding the mechanisms underlying adaptation is a ubiquitous and long-term goal in the study of all sensory systems. In this study, we took a molecular genetics approach to test a long-standing hypothesis concerning molecular mechanisms for olfactory adaptation. By mutating the previously reported phosphorylation site of ACIII in mice, we found that feedback inhibition of ACIII via Ca²⁺-induced phosphorylation on serine¹⁰⁷⁶ is not necessary for OSNs to undergo adaptation.

Thus far, three Ca²⁺-dependent negative-feedback mechanisms have been proposed for OSN adaptation. Firstly, Ca²⁺ via calmodulin (CaM) may feedback to the CNG channel, desensitizing the CNG channel to cAMP (Chen and Yau, 1994; Kurahashi and Menini, 1997). Secondly, Ca²⁺ via CaM may enhance the catalytic activity of PDE1C (Yan et al., 1995), which is enriched in OSN cilia, leading to increased cAMP degradation. Thirdly, Ca²⁺ may inhibit ACIII activity by stimulating CaMKII-mediated ACIII phosphorylation (Wei et al., 1998; Leinders-Zufall et al., 1999), decreasing cAMP synthesis. The role of CNG channel desensitization was previously shown to be unnecessary for OSN adaptation (Song et al., 2008). In the case of PDE1C (Cygnar and Zhao, 2009), the *pde1c* knockout mice show attenuated adaptation, but with reduced response amplitude at rest. Such phenotype leaves the precise role of PDE1C in adaptation unclear. In this study, we tested feedback inhibition of ACIII via Ca²⁺-induced phosphorylation. Previous studies demonstrated that serine¹⁰⁷⁶ is the only residue responsible for Ca²⁺-induced phosphorylation and inhibition of ACIII (Wei et al., 1996). We found that mice carrying a mutation of serine¹⁰⁷⁶ of ACIII to alanine do not show any defects in OSN responses when analyzed with EOG recordings, suggesting that feedback inhibition of ACIII via Ca²⁺-induced phosphorylation on serine¹⁰⁷⁶ is not necessary for OSN adaptation. The lack of adaptation defect could result from compensation from other feedback mechanisms, or this ACIII-dependent mechanism might not be involved in OSN adaptation. Nonetheless, these observations suggest that the mechanisms underlying OSN adaptation could be more complex than previously acknowledged. Future investigations into the integration of the above proposed mechanisms as well as identification of novel Ca²⁺ feedback targets should provide new insight into how OSN adaptation occurs.

It has become apparent that in vertebrate olfactory transduction cAMP is used as a trigger for Ca²⁺-mediated processes. It is Ca²⁺ that in turn dictates the amplitude and kinetics, especially pertaining to termination (Stephan et al., 2012), of the electrical response. As cAMP and Ca²⁺ are common second messengers, which operate in many cell types, knowledge gained from studying olfactory transduction could provide insight into how these

two second messenger systems interact to determine the input-output relationship of relevant cellular processes in cell types.

In addition to its well-defined role in mediating olfactory transduction in OSN cilia, ACIII has been implicated to function at OSN axonal terminals for proper development of axonal projections (Dal Col et al., 2007; Zou et al., 2007). ACIII is also expressed in several other cells and tissues (Horner et al., 2003; Livera et al., 2005; Bishop et al., 2007; Pluznick et al., 2009). For example, ACIII is localized in the cilia throughout many regions of the brain (Bishop et al., 2007). However, the physiological function of ACIII in those cells and tissues is still largely unknown. We showed in this study that ACIII phosphorylation is not required for response adaptation in OSNs. It would be interesting to investigate the physiological relevance of Ca²⁺-induced ACIII phosphorylation in other ACIII-expressing cells and tissues as well.

Acknowledgments

We thank Dr. M. Capecchi for providing the self-excising neo cassette and Drs. J. Beavo, J. Cherry and F. Margolis for providing antibodies. We thank Drs. J. Reisert, R. Kuruvilla, S. Hattar, A. Stephan and the members of the JHU Biology Mouse Tri-lab for helpful comments and discussion. This work was supported by NIH DC009946 and DC007395.

References

- Bakalyar HA, Reed RR. Identification of a specialized adenylyl cyclase that may mediate odorant detection. *Science*. 1990; 250:1403–1406. [PubMed: 2255909]
- Billig GM, Pal B, Fidzinski P, Jentsch TJ. Ca²⁺-activated Cl⁻ currents are dispensable for olfaction. *Nat Neurosci*. 2011; 14:763–769. [PubMed: 21516098]
- Bishop GA, Barbari NF, Lewis J, Mykytyn K. Type III adenylyl cyclase localizes to primary cilia throughout the adult mouse brain. *J Comp Neurol*. 2007; 505:562–571. [PubMed: 17924533]
- Boekhoff I, Kroner C, Breer H. Calcium controls second-messenger signalling in olfactory cilia. *Cell Signal*. 1996; 8:167–171. [PubMed: 8736699]
- Bunting M, Bernstein KE, Greer JM, Capecchi MR, Thomas KR. Targeting genes for self-excision in the germ line. *Genes Dev*. 1999; 13:1524–1528. [PubMed: 10385621]
- Chen TY, Yau KW. Direct modulation by Ca(2+)-calmodulin of cyclic nucleotide-activated channel of rat olfactory receptor neurons. *Nature*. 1994; 368:545–548. [PubMed: 7511217]
- Cygnar KD, Zhao H. Phosphodiesterase 1C is dispensable for rapid response termination of olfactory sensory neurons. *Nat Neurosci*. 2009; 12:454–462. [PubMed: 19305400]
- Cygnar KD, Stephan AB, Zhao H. Analyzing responses of mouse olfactory sensory neurons using the air-phase electroolfactogram recording. *J Vis Exp*. 2010
- Dal Col JA, Matsuo T, Storm DR, Rodriguez I. Adenylyl cyclase-dependent axonal targeting in the olfactory system. *Development*. 2007; 134:2481–2489. [PubMed: 17537788]
- Firestein S. How the olfactory system makes sense of scents. *Nature*. 2001; 413:211–218. [PubMed: 11557990]
- Horner K, Livera G, Hinckley M, Trinh K, Storm D, Conti M. Rodent oocytes express an active adenylyl cyclase required for meiotic arrest. *Dev Biol*. 2003; 258:385–396. [PubMed: 12798295]
- Kleene SJ. The electrochemical basis of odor transduction in vertebrate olfactory cilia. *Chem Senses*. 2008; 33:839–859. [PubMed: 18703537]
- Kurahashi T, Shibuya T. Ca²⁺-dependent adaptive properties in the solitary olfactory receptor cell of the newt. *Brain Res*. 1990; 515:261–268. [PubMed: 2113412]
- Kurahashi T, Menini A. Mechanism of odorant adaptation in the olfactory receptor cell. *Nature*. 1997; 385:725–729. [PubMed: 9034189]
- Leinders-Zufall T, Ma M, Zufall F. Impaired odor adaptation in olfactory receptor neurons after inhibition of Ca²⁺/calmodulin kinase II. *J Neurosci*. 1999; 19:RC19. [PubMed: 10407061]

- Leinders-Zufall T, Greer CA, Shepherd GM, Zufall F. Imaging odor-induced calcium transients in single olfactory cilia: specificity of activation and role in transduction. *J Neurosci*. 1998; 18:5630–5639. [PubMed: 9671654]
- Livera G, Xie F, Garcia MA, Jaiswal B, Chen J, Law E, Storm DR, Conti M. Inactivation of the mouse adenylyl cyclase 3 gene disrupts male fertility and spermatozoon function. *Mol Endocrinol*. 2005; 19:1277–1290. [PubMed: 15705663]
- Pluznick JL, Zou DJ, Zhang X, Yan Q, Rodriguez-Gil DJ, Eisner C, Wells E, Greer CA, Wang T, Firestein S, Schnermann J, Caplan MJ. Functional expression of the olfactory signaling system in the kidney. *Proc Natl Acad Sci U S A*. 2009; 106:2059–2064. [PubMed: 19174512]
- Scott JW, Scott-Johnson PE. The electroolfactogram: a review of its history and uses. *Microsc Res Tech*. 2002; 58:152–160. [PubMed: 12203693]
- Song Y, Cygnar KD, Sagdullaev B, Valley M, Hirsh S, Stephan A, Reisert J, Zhao H. Olfactory CNG channel desensitization by Ca²⁺/CaM via the B1b subunit affects response termination but not sensitivity to recurring stimulation. *Neuron*. 2008; 58:374–386. [PubMed: 18466748]
- Stephan AB, Shum EY, Hirsh S, Cygnar KD, Reisert J, Zhao H. ANO2 is the ciliary calcium-activated chloride channel that may mediate olfactory amplification. *Proc Natl Acad Sci U S A*. 2009; 106:11776–11781. [PubMed: 19561302]
- Stephan AB, Tobochnik S, Dibattista M, Wall CM, Reisert J, Zhao H. The Na⁽⁺⁾/Ca⁽²⁺⁾ exchanger NCKX4 governs termination and adaptation of the mammalian olfactory response. *Nat Neurosci*. 2012; 15:131–137. [PubMed: 22057188]
- Wayman GA, Impey S, Storm DR. Ca²⁺ inhibition of type III adenylyl cyclase in vivo. *J Biol Chem*. 1995; 270:21480–21486. [PubMed: 7665559]
- Wei J, Wayman G, Storm DR. Phosphorylation and inhibition of type III adenylyl cyclase by calmodulin-dependent protein kinase II in vivo. *J Biol Chem*. 1996; 271:24231–24235. [PubMed: 8798667]
- Wei J, Zhao AZ, Chan GC, Baker LP, Impey S, Beavo JA, Storm DR. Phosphorylation and inhibition of olfactory adenylyl cyclase by CaM kinase II in Neurons: a mechanism for attenuation of olfactory signals. *Neuron*. 1998; 21:495–504. [PubMed: 9768837]
- Wong ST, Trinh K, Hacker B, Chan GC, Lowe G, Gaggar A, Xia Z, Gold GH, Storm DR. Disruption of the type III adenylyl cyclase gene leads to peripheral and behavioral anosmia in transgenic mice. *Neuron*. 2000; 27:487–497. [PubMed: 11055432]
- Yan C, Zhao AZ, Bentley JK, Loughney K, Ferguson K, Beavo JA. Molecular cloning and characterization of a calmodulin-dependent phosphodiesterase enriched in olfactory sensory neurons. *Proc Natl Acad Sci U S A*. 1995; 92:9677–9681. [PubMed: 7568196]
- Zou DJ, Chesler AT, Le Pichon CE, Kuznetsov A, Pei X, Hwang EL, Firestein S. Absence of adenylyl cyclase 3 perturbs peripheral olfactory projections in mice. *J Neurosci*. 2007; 27:6675–6683. [PubMed: 17581954]
- Zufall F, Leinders-Zufall T. The cellular and molecular basis of odor adaptation. *Chem Senses*. 2000; 25:473–481. [PubMed: 10944513]

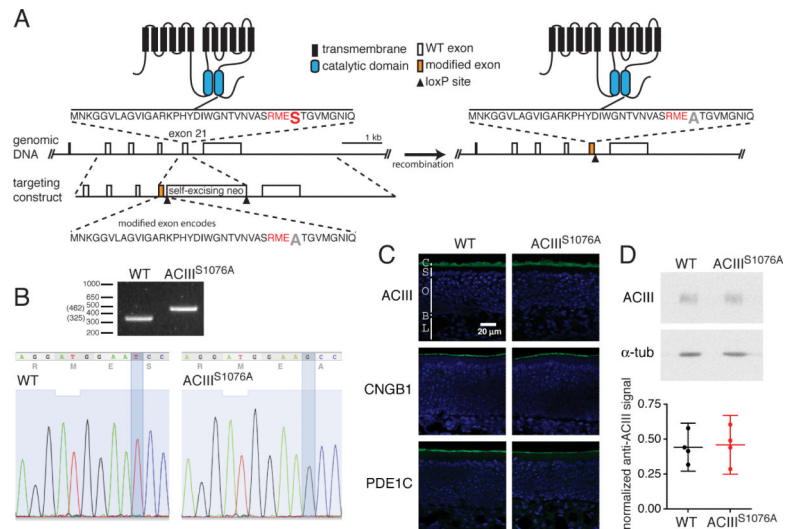


Figure 1. Generation of ACIII^{S1076A} mice

A. Illustration of the genetic targeting strategy. Left panel, showing wildtype ACIII protein structure at the top, partial *Adcy3* gene structure with open boxes representing exons in the middle, and the targeting construct at the bottom. The color filled open box in the targeting construct and in the genomic DNA on the right panel represents the modified exon 21 containing codon mutation from serine¹⁰⁷⁶ to alanine. The amino acid sequence coded by exon 21, with the CaMKII consensus sequence RMES in red and the serine¹⁰⁷⁶ in a larger font, is shown and its location in ACIII protein is indicated. Right panel, showing the corresponding modified ACIII protein and gene structure.

B. Top, PCR-based genotyping of wildtype and ACIII^{S1076A} homozygous littermates. Bottom, sequencing confirms the T to G base pair substitution in ACIII^{S1076A} mice, changing the codon of serine (TCC) to that of alanine (GCC).

C. Immunostaining on sections of olfactory epithelium (OE) for ACIII, CNGB1b and PDE1C. Sections were counterstained with DAPI (blue) to label cell nuclei. C, ciliary layer; S, supporting cell layer; O, OSN layer; B, basal lamina; L, lamina propria.

D. Top, Western blots for ACIII and α -tubulin on total OE proteins. Bottom, quantification of Western blotting. Values are normalized to α -tubulin staining and shown in arbitrary units. ACIII is detected at similar levels in wildtype and ACIII^{S1076A} mice. Each datum point represents an individual mouse. Error bars are 95% confidence intervals (CI).

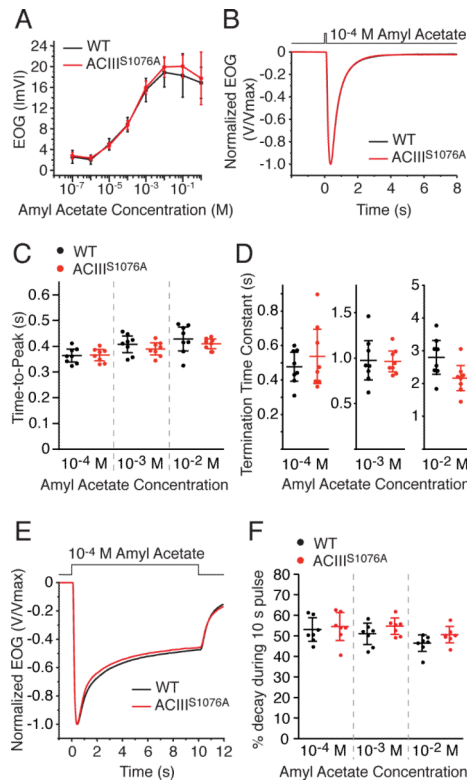


Figure 2. EOG analysis of OSN response to single odorant pulses

A to D. EOG analysis to a single 100-msec pulse of amyl acetate. **A**, Dose–response relations of EOG peak amplitude from wildtype ($n = 5$) and ACIII^{S1076A} ($n = 4$) mice. Concentrations on the X-axis are those of the liquid solution. Data points are linked with straight lines. **B**, Averaged EOG traces to 10⁻⁴ M amyl acetate (Wildtype, $n = 8$; ACIII^{S1076A}, $n = 8$). Responses are normalized with the peak given the unit for comparison of response kinetics. **C**, Time-to-peak, defined as the time from the initiation of odorant pulse to the response peak. **D**, Termination time constants, determined by a single exponential fit to the decay phase of the EOG trace.

E and F. EOG analysis to a 10-sec pulse of amyl acetate. Data are taken from the recording of the first response in the paired sustained pulse experiments shown in Fig. 3. **E**, Averaged EOG traces to 10⁻⁴ M amyl acetate (Wildtype, $n = 7$; ACIII^{S1076A}, $n = 7$). Responses are normalized with the peak given the unit for comparison of the amplitude reduction over the course of the stimulation. **F**, Amplitude reduction during stimulation, presented as the percentage of the amplitude at 10 sec to the peak. Wildtype and ACIII^{S1076A} mice show comparable amplitude reduction during the stimulation. All error bars are 95% CI.

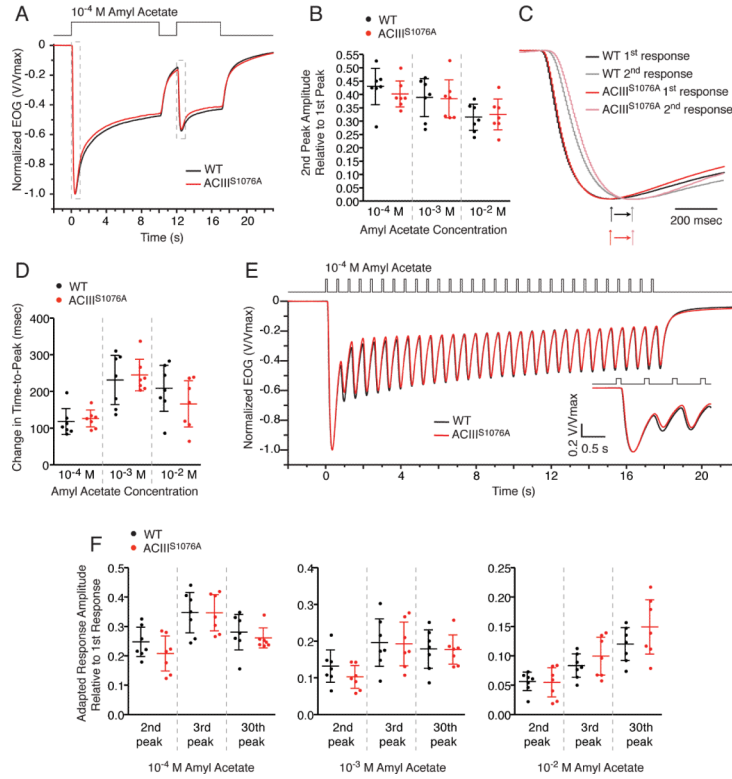


Figure 3. EOG analysis of OSN response to adaptation stimulation paradigms

A to D. EOG analysis to paired sustained (10-sec followed by 5-sec) odorant pulses with 2-sec interpulse interval. **A**, Averaged EOG traces to 10^{-4} M amyl acetate (Wildtype, $n = 7$; $ACIII^{S1076A}$, $n = 7$). Responses are normalized with the peak given the unit for comparison of amplitude reduction. The portion in dashed boxes is replotted in **C** to show the activation phase. **B**, Ratios of the second peak amplitude to the first. Because the response to the 1st odorant pulse had not decayed to baseline at the time the 2nd pulse was given, the recorded 2nd response reflected a sum of the residual 1st response and the net response to the 2nd pulse. The net peak amplitude of the second response was determined by first fitting a trace to the decay phase of the first response and subsequently subtracting the value of this trace at the peak time of the second response from the recorded second peak amplitude. Wildtype and $ACIII^{S1076A}$ mice show comparable reduction in the peak amplitude of the 2nd response. **C**, Expanded EOG traces to 10^{-4} M amyl acetate, showing the activation phase. All responses are normalized to the unit for comparison of activation kinetics. **D**, Changes in activation kinetics due to adaptation, calculated by subtraction of time-to-peaks between the 2nd response and the 1st response. Wildtype and $ACIII^{S1076A}$ mice show similarly lengthened time-to peak in the 2nd response.

E and F. EOG analysis to a train of 30 100-msec odorant pulses with 0.5-sec interpulse interval. **E**, Averaged EOG traces to 10^{-4} M amyl acetate (Wildtype, $n = 7$; $ACIII^{S1076A}$, $n = 7$). Responses are normalized with the peak given the unit for comparison of amplitude reduction and response kinetics. Responses to the first three pulses are expanded in inset. **F**, Ratios of the second, third and thirtieth peak amplitude to the first. The net response amplitude to a given pulse is calculated by subtracting the residual response of the previous pulse from the recorded response, similarly as described in **B**. To each given pulse from the 2nd through the 30th, wildtype and $ACIII^{S1076A}$ mice show comparable amplitude ratio to the first.

All error bars are 95% CI.